



Short communication

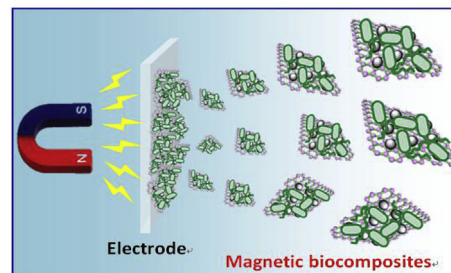
Magnet-assisted rapid and controllable construction of an electroactive biofilm for microbial current generation

Lihua Zhou^a, Yi Wang^b, Lihua Sun^a, Bin Tan^b, Xiaoshan Luo^b, Yong Yuan^{b,*}^a Institute of Natural Medicine & Green Chemistry, School of Chemical Engineering and Light Industry, Guangdong University of Technology, Guangzhou, 510006, China^b Institute of Environmental Health and Pollution Control, School of Environmental Science and Engineering, Guangdong University of Technology, Guangzhou, 510006, China

HIGHLIGHTS

- *G. sulfurreducens* was captured by magnetically active N-doped Fe₃O₄/rGO.
- The biocomposite was brought onto the electrode by means of external magnetic field.
- Maximum current density was 0.24 ± 0.07 mA/cm² for N-M/rGO-captured biofilm.
- The magnetically active biofilm was efficient for microbial energy harvesting.

GRAPHICAL ABSTRACT



ARTICLE INFO

Keywords:

Electroactive biofilm
Bacterial capture
Magnet
Microbial current generation

ABSTRACT

Artificial electroactive biofilms have been developed as potential alternative to natural biofilms because the fabrication of them is simple, rapid, standardized and controllable. However, the construction of artificial electroactive biofilms usually involves cell dry process or the use of binding agents, which inevitably decreases the viability of the entrapped cells. Herein, a fast and convenient bacterial immobilization method is proposed as an attempt to construct an artificial electroactive biofilm for microbial energy harvesting, in which bacteria are captured by magnetically active nitrogen-doped Fe₃O₄/reduced graphene oxide composite and bring onto the electrode by means of external magnetic field. The resulting artificial electroactive biofilm produces higher current than the natural electroactive biofilm in the bioelectrochemical systems. The improved performance of the biofilm captured by nitrogen-doped Fe₃O₄/reduced graphene oxide can be attributed to its high surface, high affinity for the attachment of *Geobacter sulfurreducens*, and efficient extracellular electron transfer between microbial biofilm and electrode. Moreover, because of the magnetic activity of the resulting electroactive biofilm, the current produced from the artificial electroactive biofilm is magnetically switchable. This study offers a new approach to rapidly fabricate an artificial electroactive biofilm and provides an opportunity for the fabrication of a magnetically controllable microbial bioelectrochemical system.

1. Introduction

Electroactive bacteria, a group of microorganisms that is capable of transferring electrons outside of their cellular environment, have

attracted considerable interest [1]. They are believed not only to play a key role in environmental redox cycles [2], but also in microbial bioelectrochemical systems (BESs) for capturing energy from organic waste, microbial electrosynthesis, biosensors and biocomputing [3–5].

* Corresponding author.

E-mail address: yuan Yong@soil.gd.cn (Y. Yuan).<https://doi.org/10.1016/j.jpowsour.2018.09.089>

Received 22 May 2018; Received in revised form 17 September 2018; Accepted 27 September 2018

Available online 02 October 2018

0378-7753/ © 2018 Elsevier B.V. All rights reserved.

In the BESs, electroactive bacteria can intentionally attach to the surface of electrodes to form electroactive biofilms (EABs) [6]. Electroactive bacteria attach to solid electrodes with high local cell density, shorter extracellular electron transfer (EET) distance, and the involvement of direct electron transfer pathways, resulting in an efficient EET superior to that of planktonic bacteria [7]. However, it was observed that the EET of the EABs could suffer from the diffusion of substrate because the diffusion factor is more influential than the rate of reaction of the biofilm at a certain thickness and density [8,9]. In view of this, great efforts have been paid to construct efficient EABs for high-performance BESs [10,11].

In general, the biofilm formation is a complex process that involves the bacterial adhesion to a substrate surface and cell–cell adhesion to form multiple layers of the biofilm. It is usually time-intensive, taking from several days to several months, to build up a mature biofilm on a surface [12]. In BESs, electroactive bacterial cells are capable of being enriched on the electrodes under constant bias potential or external resistance to form EABs, which were defined herein as natural EABs. Similarly, the natural EABs grown on the electrode surface require periods of time that can vary from days to weeks before reaching an optimal electrode response [13,14]. Besides, natural EABs usually have limited thickness varying from several to tens of microns due to the diffusion limitation of substrates and insufficient interaction of bacteria with electrodes, which impede further improvement of the EET efficiency [15,16]. In this regard, artificial EABs based on cell encapsulation approaches have been considered good alternatives to natural EABs, which have been performed by embedding planktonic bacteria into exogenous materials such as silica gel, graphite/polypyrrole, carbon nanotube, and carbon nanoparticles [17–20]. The resulting EABs showed remarkable EET efficiency in the BESs. In addition, the resulting EABs offer a stable and defined microbial community, facilitating electrochemical studies on a standardized platform. However, current approaches used either cell dry process or binding agents (i.e. polytetrafluoroethylene, PTFE) to fix the artificial biofilm on the electrode surface, which inevitably decrease the viability of the entrapped cells or cause cell damage [21,22].

In a study by Lee et al. [23], glucose oxidase was immobilized in a nanostructured magnetic material to fabricate an enzyme-based biocomposite, which was brought into contact with the electrode by means of a magnet to construct a magnetically switchable bioelectrocatalytic system. Magnetic materials have been proven to be also efficient for capture bacterial cells, which were usually used to remove bacterial cells from various waters [24–26]. However, this concept has not yet been used to rapidly construct living and controllable EABs. Herein, we demonstrated the use of a magnetic material (N-doped Fe_3O_4 /reduced graphene oxide, N-M/rGO) to capture *Geobacter sulfurreducens* cells for forming biocomposites, which was brought into contact with the electrode by a magnet to form an artificial EAB. The morphology and electrochemical characterizations of the resulting biofilms were evaluated. The magnetically switchable bioelectrocatalytic property of the biofilm was also revealed.

2. Experiments

2.1. Bacterial strain

Geobacter sulfurreducens strain PCA (ATCC51573) was sub-cultured using a standard anaerobic conditions with freshwater medium containing fumarate (40 mM) and acetate (10 mM) at 30 °C using previously described methods [27]. This anaerobic medium contains (per 1 L): 0.25 g NH_4Cl , 0.1 g KCl , 0.6 g $\text{NaH}_2\text{PO}_4 \cdot \text{H}_2\text{O}$, 2.5 g NaHCO_3 , 10 mL of a mineral mixture, and 10 mL of vitamin mixture. The medium solution was flushed with N_2/CO_2 (80/20, v/v) for 30 min prior to sealing with butyl rubber stoppers. The log-phase cells are harvested, centrifuged and re-suspended in sterile water for further use.

2.2. Preparation of magnetic N-doped Fe_3O_4 /rGO

Graphene oxide (GO) was prepared from natural graphite flakes using a modified Hummers method [28]. N-M/rGO was prepared by using previously described methods [29]. In a typical experiment, a 6 mL GO (1.5 mg/mL) aqueous dispersion with the iron (II) acetate (20 mg) was firstly sonicated for 10 min, and then 20 mg polypyrrole was slowly added to form a stable complex solution by sonication for 10 min. Subsequently, the stable suspension was sealed in a Teflon-lined stainless steel vessel and treated at 180 °C for 12 h, and then the as-prepared solid product was heat-treated at 600 °C for 3 h in N_2 gas. Notably, the polypyrrole was used as the carbon and nitrogen sources to produce a N-doped carbon material that was associated with the resulting Fe_3O_4 nanoparticles/reduced graphene oxide sheets composite (Fe_3O_4 /rGO, denoted as M/rGO). For comparison, we also prepared Fe_3O_4 /rGO via the same procedure, but the polypyrrole was not added during the synthesis. The as-prepared magnetic N-M/rGO (10.0 mg) was suspended in the as-prepared 5 mL of anaerobic *G. sulfurreducens* suspension (1.0 OD), which was subsequently incubated at 30 °C for 60 min to produce a biocomposite.

2.3. Bacterial capture efficiency of N-M/rGO

The bacterial concentration was adjusted to a desired level (1.0 OD), a certain amount of N-M/rGO (5.0 mg) suspended in PBS (50 mM) was then added into the bacterial solution, and the solution volume was fixed to 5.0 mL. The solution was incubated by a rotary shaker at 300 rpm for a specific time period (0–60 min). An external magnet was employed for magnetic separation after the suspension was allowed to settle for a specific period. The supernatant was then carefully pipetted into a cell to measure its OD using absorption spectroscopy. The relative efficiencies of the magnetic capture of bacteria by N-M/rGO were calculated from the decrease of turbidity relative to a reference before magnetic capture [24,25].

2.4. BES fabrication and inoculation

A single-chamber three-electrode system, in which a tin-doped In_2O_3 (ITO) working electrode (exposed surface area of 5 cm^2) was glued to an open-topped of cylindrical container (40 mL) with epoxy resin, as illustrated in Fig. S1, was used for the electrochemical studies of the EABs. In the reactor, an Ag/AgCl reference electrode (CHI111, Shanghai Chenhua Apparatus Co., China) was placed in the center, and a coiled titanium wire electrode (diameter of 2.0 mm and surface area of 0.8 cm^2) was used as the counter electrode. The BES was inoculated with 5 mL of the as-prepared N-M/rGO/*G. sulfurreducens* biocomposite and filled with freshwater medium containing acetate (10 mM) only as the electron donor. The working electrode was held at 0.2 V (vs. Ag/AgCl) by a multichannel potentiostat (CHI1000C, Shanghai Chenhua Apparatus Co., China) and served as the electron acceptor. Magnetic on-off switching of biofilm electrode was conducted by alternate positioning of the magnet close to or far away from the ITO electrode (Fig. S1). The current density was normalized by the working electrode surface area. All of the tests were conducted in triplicate, and the mean \pm standard deviation values were reported.

2.5. Analytical techniques

The XPS spectra were recorded on an X-ray photoelectron spectrometer (Kratos Model XSAM800) with a monochromatic Mg 300 W X-ray source. Scanning electron microscopy (SEM) images were observed by SEM (JEOL, JSM-6330F; Japan) at 20 kV. The LIVE/DEAD BacLight viability kit (L7012, Thermo Fisher Scientific, USA) was applied to identify the bacteria viability using a laser confocal scanning microscope (CLSM, Leica TCS-SP2, Germany). The X-ray diffraction (XRD)

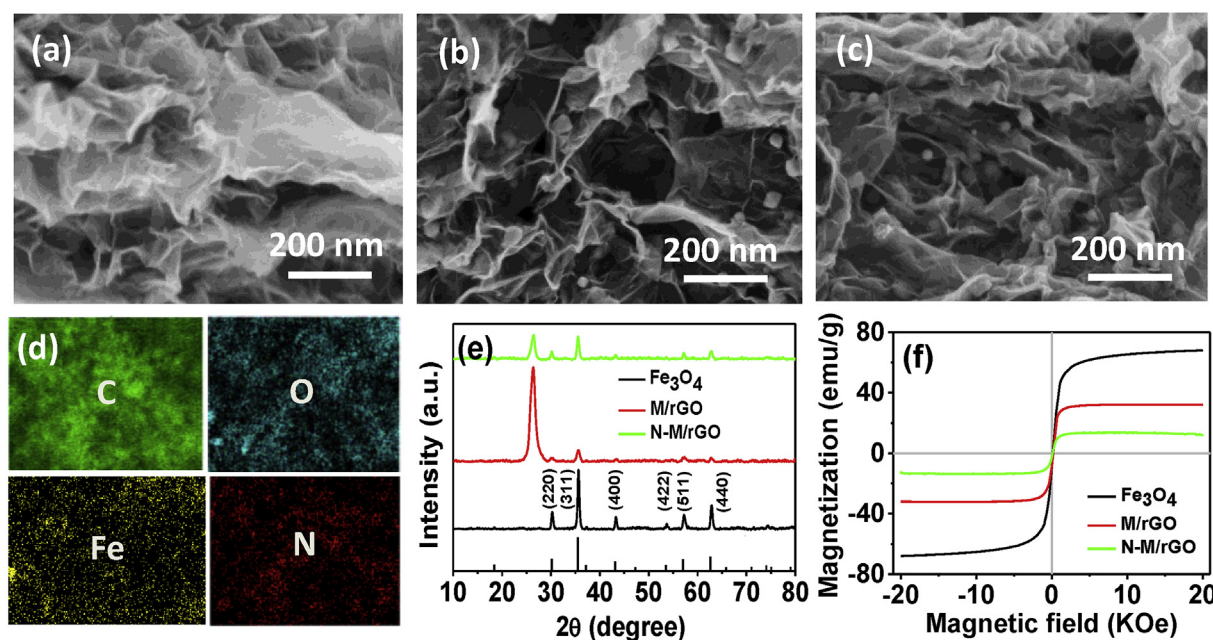


Fig. 1. SEM images of rGO (a), M/rGO (b), N-M/rGO (c); (d) SEM-EDS mapping of N-M/rGO; (e) XRD patterns of Fe_3O_4 , M/rGO, and N-M/rGO; (f) room temperature magnetization curves of Fe_3O_4 , M/rGO, and N-M/rGO.

patterns of samples were recorded via an X-ray diffractometer (XRD, Philips X'pert Pro MPD, PANalytical, The Netherlands) with $\text{CuK}\alpha$ radiation ($\gamma = 0.154 \text{ nm}$). The magnetic properties of the nanoparticles were studied using a vibrating sample magnetometer (LDJ 9600-1, USA). Cyclic voltammograms (CVs) of the biofilm electrodes were performed by scanning the potential between 0.2 and -0.8 V vs. Ag/AgCl with a scan rate of 5 mV/s . The CV scans of the biofilm electrodes were performed in both turnover (in the presence of acetate) and non-turnover (in the absence of acetate) conditions. For non-turnover CV measurements, the electrolyte was not amended with nutrition and mineral solutions to avoid interference.

3. Results and discussion

3.1. Characterization of N-M/rGO

The structure and morphology of as-prepared N-M/rGO were investigated by the SEM scans. As shown in Fig. 1a, the rGO showed typical structure with randomly aggregated, thin, and crumpled sheets with a worm-like appearance. The decoration of Fe_3O_4 nanoparticles on the graphene sheets was observed on the M/rGO and N-M/rGO composites (Fig. 1b and c). It is noteworthy that the morphology of the M/rGO and N-M/rGO was almost identical, indicating that the use of polypyrrole during the synthesis process did not affect the structure of the graphene and the formation of Fe_3O_4 nanoparticles. The elemental mapping analysis of the as-prepared N-M/rGO suggested the presence of C, O, N, and Fe components in the composite (Fig. 1d). Notably, the N is distributed on both the region of Fe_3O_4 nanoparticles and graphene layers, indicating that Fe-N-C active sites have been established at the interface of Fe_3O_4 nanoparticles. The XPS survey also showed the presence of C, O, N, and Fe components in the composite (Fig. S2). The high-resolution O 1s can be separated into three peaks with the anionic oxygen in Fe-O (at 529.7 eV), the carbonyl oxygen in C=O (at 531.4 eV), and the oxygen in C-O (at 533.0 eV) [30], respectively. The high-resolution N 1s scan indicated that presence of four forms of nitrogen, namely, pyridinic, pyrrolic, graphitic and oxidized N, respectively. The high-resolution Fe 2p scan showed two peaks at 724.5 and 710.6 eV , which could be assigned to $\text{Fe } 2p_{1/2}$ and $\text{Fe } 2p_{3/2}$ for Fe_3O_4 [31], respectively. The XRD pattern further confirmed the

formation of Fe_3O_4 in the composite (JCPDS PDF#63-3107) (Fig. 1e). Compared with pure Fe_3O_4 , the XRD patterns of M/rGO and N-M/rGO showed an extra largely shoulder centered at 25° , which can be attributed to the presence of graphene [32]. To evaluate the magnetic separation capacity of the as-prepared samples, the magnetic hysteresis loops of pure Fe_3O_4 , M/rGO, and N-M/rGO were conducted at room temperature (Fig. 1f). It is noteworthy that the magnetic saturation value of the pure Fe_3O_4 nanoparticles was higher than those of M/rGO and N-M/rGO, which is due to the sharply reduced relative content of Fe_3O_4 [33]. As shown in Fig. S1, the N-M/rGO composite can be separated from the black and stable suspension solution with a help of an external magnet, suggesting that the magnetic separation capacity of the N-M/rGO was still strong enough to separate them.

3.2. Cell capture properties of N-M/rGO

The as-prepared magnetic N-M/rGO was employed in the BES to assist the rapid construction of a magnetically switchable EAB (Fig. S1). The operating principle is illustrated in Fig. 2a. Current was generated by electron transfer from bacterial cells to the electrode when the bacterial cells captured by N-M/rGO in a solution containing substrate (acetate) were brought into contact with the ITO electrode by means of a magnet placed close to the electrode, which represented a state of switched “on” for the microbial energy harvesting. Conversely, when the magnet was placed under the bottom of the reactor, the N-M/rGO/cell biofilm was removed away from the working electrode, inducing that the current was decreased to background level (switched “off”). The current could be reversibly switched back and forth between the on and off states by alternating the position of the external magnet, which could benefit the fabrications of microorganism-based biosensors, bioelectronics and biofuel cells [34,35]. In this regard, the cell capture ability of the magnetic materials was investigated by SEM and CLSM measurements. The SEM images of Fig. 2b–d showed that pure rGO, M/rGO, and N-M/rGO were all capable of capturing bacterial cells, but the ability of the cell capture varied among these materials. More bacterial cells were obviously observed in the M/rGO and N-M/rGO frameworks than that in the rGO, suggesting that these two composites were more feasible to capture bacterial cells. Compared with the M/rGO, more cells were captured in the N-M/rGO, which was likely due to the N

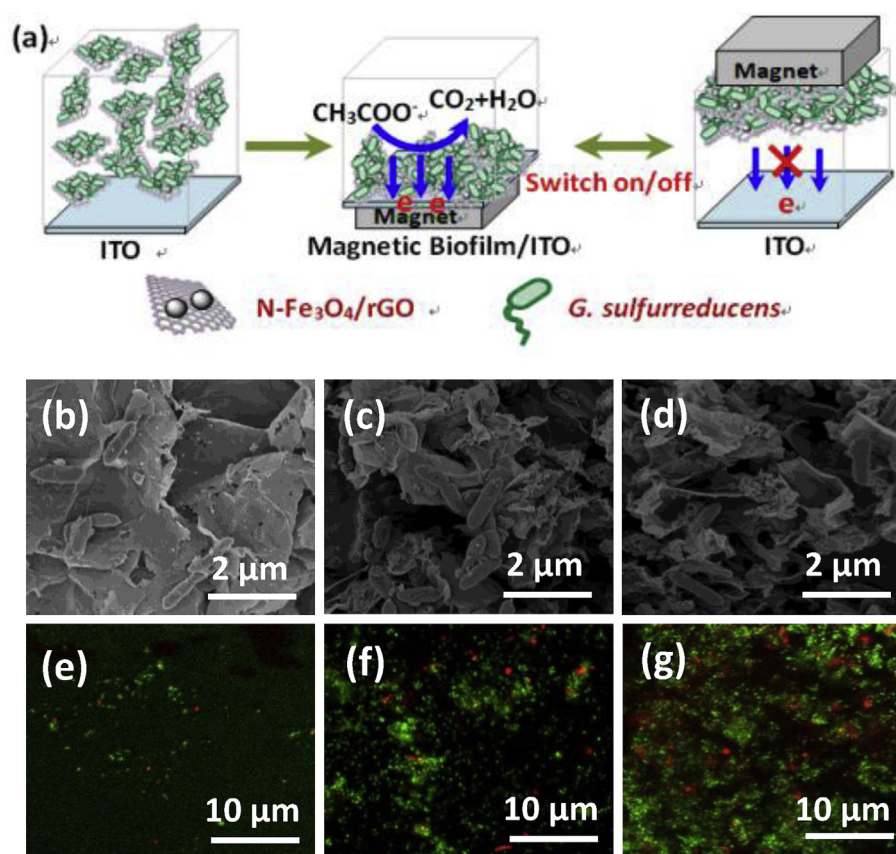


Fig. 2. (a) Schematic illustration of the magnet assisted construction of N-M/rGO/*G. sulfurreducens* composite film on the ITO electrode for current generation; SEM images of rGO/*G. sulfurreducens* (b), M/rGO/*G. sulfurreducens* (c), and N-M/rGO/*G. sulfurreducens* (d) biocomposites, respectively; Confocal fluorescent images of live (green) and dead (red) bacterial cells in the biocomposites: rGO/*G. sulfurreducens* (e), M/rGO/*G. sulfurreducens* (f), and N-M/rGO/*G. sulfurreducens* (g) biocomposites. (For interpretation of the references to colour in this figure legend, the reader is referred to the Web version of this article.)

doping in the N-M/rGO. The N doping can create more positive charged sites on the surface of the N-M/rGO, which can benefit the adsorption of negatively charged cells on the surface of this material [36,37]. Fluorescent-based cell live/dead test of live and dead bacterial cells were confirmed the presence of living cells in the biocomposites (Fig. 2e–g). As measured, over 90% of cells could be captured by N-M/rGO, while only 75% of cells in the suspension could be captured by M/rGO in 30 min (Fig. S3). The CLSM viability staining indicated that 90%, 88% and 80% of the cells were viable in the biofilms captured by rGO, M/rGO and N-M/rGO, respectively, demonstrating the good biocompatibility of these materials. In order to determine the bacterial cell density, protein was extracted from the biocomposites. The biomass density in the capture materials was determined to be 0.02 ± 0.01 , 0.08 ± 0.02 and 0.17 ± 0.02 mg of protein/mg (rGO-based material) for rGO, M/rGO and N-M/rGO, respectively.

3.3. Current generation of the magnetically and electrochemically active biofilm

The electrocatalytic activity of the EAB constructed with the aid of an external magnet was evaluated by recording the current generation in the BES. Prior to constructing the artificial EAB, the M/rGO/*G. sulfurreducens* and N-M/rGO/*G. sulfurreducens* biocomposites were prepared by inoculating the mixture of magnetic materials and cells for 1.0 h. As shown in Fig. 3a, almost no current was observed at initial from the BESs inoculated with M/rGO/*G. sulfurreducens*, and N-M/rGO/*G. sulfurreducens* biocomposites in the absence of an external magnet. However, the current was immediately generated from the BESs as the external magnet was placed close the working electrode, demonstrating the feasibility of the construction of EABs with the proposed method. It is noteworthy that the maximum current density (0.24 ± 0.07 mA/cm²) of the N-M/rGO/*G. sulfurreducens* biofilm was higher than that of the M/rGO/*G. sulfurreducens* (0.13 ± 0.03 mA/cm²), which could be

due to the more efficient cell capture ability of the N-M/rGO. The biomass density in the N-M/rGO/*G. sulfurreducens* biofilm was 0.17 ± 0.01 , 0.24 ± 0.03 and 0.28 ± 0.03 mg of protein/mg N-M/rGO at 0, 60 and 120 h after the acetate was added to the reactor. The slight increase in the biomass density demonstrated the growth of the cells occurred on the electrode, which indicated that the cells could be attached stably on the electrode by means of external magnetic field. As a result of the cell growth, a slow increase in the current was observed from the M/rGO/*G. sulfurreducens* biofilm. On the contrary, a slow decrease in the current at the M/rGO-based biofilm was observed, indicating that this biofilm was unstable due to less efficient cell capture ability of this material. The current could be also generated from the natural biofilm that was formed by inoculating the BES with only *G. sulfurreducens*, but the current only gradually increased, and it took more than 70 h to reach an optimal current. The turnover and non-turnover CV scans confirmed that the current generation was achieved from the decomposing of acetate by the EABs (Fig. S4). The N-M/rGO biofilm produced a higher current density than the natural biofilm (0.11 ± 0.02 mA/cm²), suggesting that the N-M/rGO not only assisted the biofilm formation but also facilitated the EET. A large specific surface area is considered to be essential property of a high-performance bioelectrode for the BESs [38]. In this regard, the surface area of the ITO planar electrode was increased by the attachment of N-M/rGO, which could contribute to the higher current density of the N-M/rGO biofilm. In addition, the presence of Fe₃O₄ nanoparticles might facilitate the EET because they could increase the affinity of bacterial cells to the electrode and serve as electron conduits for the EET [39,40]. As expected, the constructed biofilm was capable of being used for the fabrication of a magnetically switchable bioelectrochemical system. As shown in Fig. 3b, the current was alternately repeated in the on and off state by cyclic placement of the magnet close to and far away from the working electrode in the both N-M/rGO- and M/rGO-based BESs. Very small current responses were observed from the abiotic N-M/rGO and

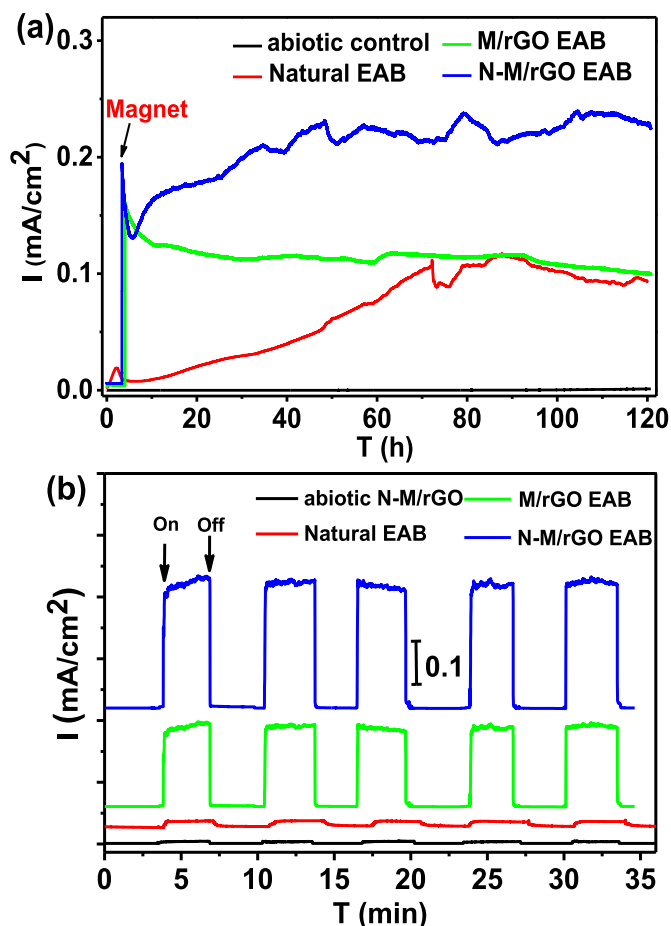


Fig. 3. (a) Current output over time in BESs with various electrodes assisted by magnet; (b) magneto-switched current generation in the BESs with various cell capture materials.

the natural EAB, which confirmed that the on-off switch of current was caused by the biocomposites rather than the solo EAB or N-M/rGO.

4. Conclusions

In this study, we have successfully demonstrated the feasibility of using magnetically active rGO-based materials to capture bacterial cells and the further use for rapid constructing efficient EABs with the aid of an external magnet. Such operation was simple and less harmful to cell compared with those reported methods for forming artificial biofilms. As a result of high surface area and high affinity of the capture materials toward bacterial cells, the constructed artificial EAB produced higher current density than the natural EAB. Moreover, the artificial EAB controlled by means of the external magnetic field could be used for the fabrication of a magnetically switchable bioelectrochemical system. The approach proposed by this study will find various applications in bioconversion, biosensors, biocomputing and switchable biofuel cells.

Acknowledgements

This work was financially supported by the Guangzhou City Science-Technology Project (No. 201707010250), the National Natural Science Foundation of China (NOs. 51678162, 41877045, and 21876032), and the Major Scientific Project of Guangdong University (No. 2017KZDXM029).

Appendix A. Supplementary data

Supplementary data to this article can be found online at <https://doi.org/10.1016/j.jpowsour.2018.09.089>.

References

- [1] L. Shi, H. Dong, G. Reguera, H. Beyenal, A. Lu, J. Liu, H. Yu, J.K. Fredrickson, Extracellular electron transfer mechanisms between microorganisms and minerals, *Nat. Rev. Microbiol.* 14 (2016) 651–662.
- [2] D.R. Lovley, E.J. Phillips, Y.A. Gorby, E.R. Landa, Microbial reduction of uranium, *Nature* 350 (1991) 413–416.
- [3] B.E. Logan, K. Rabaey, Conversion of wastes into bioelectricity and chemicals by using microbial electrochemical technologies, *Science* 337 (2012) 686–690.
- [4] A. PrévotEAU, K. Rabaey, Electroactive biofilms for sensing: reflections and perspectives, *ACS Sens.* 2 (2017) 1072–1085.
- [5] Y. Yuan, S.G. Zhou, J. Zhang, L. Zhuang, G.Q. Yang, S. Kim, Multiple logic gates based on reversible electron transfer of self-organized bacterial biofilm, *Electrochem. Commun.* 18 (2012) 62–65.
- [6] A.P. Borole, G. Reguera, B. Ringeisen, Z.W. Wang, Y. Feng, B.H. Kim, Electroactive biofilms: current status and future research needs, *Energy Environ. Sci.* 4 (2011) 4813–4834.
- [7] Y.C. Yong, Y.Y. Yu, X.H. Zhang, H. Song, Highly active bidirectional electron transfer by a self-assembled electroactive reduced-graphene-oxide-hybridized biofilm, *Angew. Chem. Int. Ed.* 53 (2014) 4480–4483.
- [8] D. Sun, J. Chen, H. Huang, W. Liu, Y. Ye, S. Cheng, The effect of biofilm thickness on electrochemical activity of *Geobacter sulfurreducens*, *Int. J. Hydrogen Energy* 41 (2016) 16523–16528.
- [9] E. Atci, J.T. Babauta, S.T. Sultana, H. Beyenal, Microbiosensor for the detection of acetate in electrode-respiring biofilms, *Biosens. Bioelectron.* 81 (2016) 517–523.
- [10] K. Guo, S. Freguia, P.G. Dennis, X. Chen, B.C. Donose, J. Keller, J.J. Gooding, K. Rabaey, Effects of surface charge and hydrophobicity on anodic biofilm formation, community composition, and current generation in bioelectrochemical systems, *Environ. Sci. Technol.* 47 (2013) 7563–7570.
- [11] Q. Du, T. Li, N. Li, X. Wang, Protection of electroactive biofilm from extreme acid shock by polydopamine encapsulation, *Environ. Sci. Technol. Lett.* 4 (2017) 345–349.
- [12] E. Tsagkari, W. Sloan, Turbulence accelerates the growth of drinking water biofilms, *Bioproc. Biosyst. Eng.* 41 (2018) 757–770.
- [13] J.C. Biffinger, J. Pietron, R. Ray, B. Little, B.R. Ringeisen, A biofilm enhanced miniature microbial fuel cell using *Shewanella oneidensis* DSP10 and oxygen reduction cathodes, *Biosens. Bioelectron.* 22 (2007) 1672–1679.
- [14] Y. Yuan, S.G. Zhou, N. Xu, L. Zhuang, Microorganism-immobilized carbon nanoparticle anode for microbial fuel cells based on direct electron transfer, *Appl. Microbiol. Biotechnol.* 89 (2011) 1629–1635.
- [15] H.S. Lee, C.I. Torres, B.E. Rittmann, Effects of substrate diffusion and anode potential on kinetic parameters for anode-respiring bacteria, *Environ. Sci. Technol.* 43 (2009) 7571–7577.
- [16] K.P. Nevin, H. Richter, S.F. Covalla, J.P. Johnson, T.L. Woodard, A.L. Orloff, H. Jia, M. Zhang, D.R. Lovley, Power output and coulombic efficiencies from biofilms of *Geobacter sulfurreducens* comparable to mixed community microbial fuel cells, *Environ. Microbiol.* 10 (2008) 2505–2514.
- [17] H.R. Luckarift, S.R. Sizemore, J. Roy, C. Lau, G. Gupta, P. Atanassov, G.R. Johnson, Standardized microbial fuel cell anodes of silica-immobilized *Shewanella oneidensis*, *Chem. Commun.* 46 (2010) 6048–6050.
- [18] Y.Y. Yu, H.L. Chen, Y.C. Yong, D.H. Kim, H. Song, Conductive artificial biofilm dramatically enhances bioelectricity production in *Shewanella*-inoculated microbial fuel cells, *Chem. Commun.* 47 (2011) 12825–12827.
- [19] S. Pinck, M. Etienne, M. Dossot, F.P. Jorand, A rapid and simple protocol to prepare a living biocomposite that mimics electroactive biofilms, *Bioelectrochemistry* 118 (2017) 131–138.
- [20] Y. Yuan, J. Ahmed, L.H. Zhou, B. Zhao, S. Kim, Carbon nanoparticles-assisted mediator-less microbial fuel cells using *Proteus vulgaris*, *Biosens. Bioelectron.* 27 (2011) 106–112.
- [21] P.G. Rouxhet, J.L. Van Haecht, J. Didelez, P. Gérard, M. Briquet, Immobilization of yeast cells by entrapment and adhesion using siliceous materials, *Enzym. Microb. Technol.* 3 (1981) 49–54.
- [22] P.Y. Yang, T. Ma, T.S. See, N. Nitisoravut, Applying entrapped mixed microbial cell techniques for biological wastewater treatment, *Water Sci. Technol.* 29 (1994) 487.
- [23] J. Lee, D. Lee, E. Oh, J. Kim, Y.P. Kim, S. Jin, H.S. Kim, Y. Hwang, J.H. Kwak, J.G. Park, Preparation of a magnetically switchable bio-electrocatalytic system employing cross-linked enzyme aggregates in magnetic mesocellular carbon foam, *Angew. Chem.* 117 (2005) 7593–7598.
- [24] Y.J. Jin, F. Liu, C. Shan, M.P. Tong, Y.L. Hou, Efficient bacterial capture with amino acid modified magnetic nanoparticles, *Water Res.* 50 (2014) 124–134.
- [25] Y.F. Huang, Y.F. Wang, X.P. Yan, Amine-functionalized magnetic nanoparticles for rapid capture and removal of bacterial pathogens, *Environ. Sci. Technol.* 44 (2010) 7908–7913.
- [26] H.W. Gu, P.L. Ho, K.W. Tsang, L. Wang, B. Xu, Using biofunctional magnetic nanoparticles to capture vancomycin-resistant enterococci and other gram-positive bacteria at ultralow concentration, *J. Am. Chem. Soc.* 125 (2003) 15702–15703.
- [27] S.M. Strycharz, A.P. Malanoski, R.M. Snider, H. Yi, D.R. Lovley, L.M. Tender, Application of cyclic voltammetry to investigate enhanced catalytic current generation by biofilm-modified anodes of *Geobacter sulfurreducens* strain DL1 vs.

- variant strain KN400, *Energy Environ. Sci.* 4 (2011) 896–913.
- [28] W.S. Hummers Jr., R.E. Offeman, Preparation of graphitic oxide, *J. Am. Chem. Soc.* 80 (1958) 1339–1339.
- [29] Z.S. Wu, S.B. Yang, Y. Sun, K. Parvez, X.L. Feng, K. Müllen, 3D nitrogen-doped graphene aerogel-supported Fe₃O₄ nanoparticles as efficient electrocatalysts for the oxygen reduction reaction, *J. Am. Chem. Soc.* 134 (2012) 9082–9085.
- [30] L.H. Zhou, C.L. Yang, J. Wen, P. Fu, Y.P. Zhang, J. Sun, H.Q. Wang, Y. Yuan, Soft-template assisted synthesis of Fe/N-doped hollow carbon nanospheres as advanced electrocatalysts for the oxygen reduction reaction in microbial fuel cells, *J. Mater. Chem.* 5 (2017) 19343–19350.
- [31] W.F. Chen, S.R. Li, C.H. Chen, L.F. Yan, Self-assembly and embedding of nanoparticles by in situ reduced graphene for preparation of a 3d graphene/nanoparticle aerogel, *Adv. Mater.* 23 (2011) 5679–5683.
- [32] J. Cheng, M. Zhang, G. Wu, X. Wang, J. Zhou, K. Cen, Photoelectrocatalytic reduction of CO₂ into chemicals using Pt-modified reduced graphene oxide combined with Pt-modified TiO₂ nanotubes, *Environ. Sci. Technol.* 48 (2014) 7076–7084.
- [33] S.H. Zhan, D.D. Zhu, S.L. Ma, W.C. Yu, Y.N. Jia, Y. Li, H.B. Yu, Z.Q. Shen, Highly efficient removal of pathogenic bacteria with magnetic graphene composite, *ACS Appl. Mater. Interfaces* 7 (2015) 4290–4298.
- [34] M. Zhou, S.J. Dong, Bioelectrochemical interface engineering: toward the fabrication of electrochemical biosensors, biofuel cells, and self-powered logic biosensors, *Acc. Chem. Res.* 44 (2011) 1232–1243.
- [35] E. Katz, I. Willner, A biofuel cell with electrochemically switchable and tunable power output, *J. Am. Chem. Soc.* 125 (2003) 6803–6813.
- [36] M.A. TerAvest, Z. Li, L.T. Angenent, Bacteria-based biocomputing with cellular computing circuits to sense, decide, signal, and act, *Energy Environ. Sci.* 4 (2011) 4907–4916.
- [37] A.H. Lu, Y. Li, S. Jin, H.R. Ding, C.P. Zeng, X. Wang, C.Q. Wang, Microbial fuel cell equipped with a photocatalytic rutile-coated cathode, *Energy Fuels* 24 (2009) 1184–1190.
- [38] J. Tang, S. Chen, Y. Yuan, X. Cai, S. Zhou, In situ formation of graphene layers on graphite surfaces for efficient anodes of microbial fuel cells, *Biosens. Bioelectron.* 71 (2015) 387–395.
- [39] R. Song, C. Zhao, L. Jiang, E. Abdel-Halim, J. Zhang, J. Zhu, Bacteria-affinity 3D macroporous Graphene/MWCNTs/Fe₃O₄ foams for high-performance microbial fuel cells, *ACS Appl. Mater. Interfaces* 8 (2016) 16170–16177.
- [40] F. Liu, A.E. Rotaru, P.M. Shrestha, N.S. Malvankar, K.P. Nevin, D.R. Lovley, Magnetite compensates for the lack of a pilin-associated c-type cytochrome in extracellular electron exchange, *Environ. Microbiol.* 17 (2015) 648–655.